Original Article

Region-specific Transcriptomic Signatures in Alzheimer's Disease: A Meta-analysis of Vulnerable Brain Regions Reveals MicroRNA–hub Gene Regulatory Networks

Khojaste Rahimi Jaberi[1], Shayan Khalili Alashti[2], Sedighe Hooshmandi[3], Pooya Vatankhah[4], Maryam Rohani Haghighi[5], Amir Savardashtaki[6], Hadi Aligholi[1], Abbas Rahimi Jaberi[1,5]

[1]Department of Neuroscience, School of Advanced Medical Sciences and Technologies, Shiraz University of Medical Sciences, Shiraz, Iran, [2]Epilepsy Research Center, Shiraz University of Medical Sciences, Shiraz, Iran, [3]Department of Radiology, School of Medicine, Medical Imaging Research Center, Shiraz, Iran, [4]Shiraz Transplant Research Center, Abu-Ali Sina Hospital, Shiraz University of Medical Sciences, Shiraz, Iran, [5]Department of Neurology, School of Medicine, Clinical Neurology Research Center, Shiraz, Iran, [6]Department of Medical Biotechnology, School of Advanced Medical Sciences and Technologies, Shiraz University of Medical Sciences, Shiraz, Iran

Address for correspondence:
Dr. Abbas Rahimi Jaberi, Department of Neurology, School of Medicine, Shiraz University of Medical Sciences, Shiraz, Iran.
E-mail: rahimijaberia@gmail.com

Abstract

Background: Alzheimer's disease (AD) is characterized by progressive neurodegeneration in regionally vulnerable brain areas, yet molecular insights into early pathogenic mechanisms remain limited. **Methods:** We conducted a meta-analysis of transcriptomic datasets from brain regions affected in early-to-moderate AD – including entorhinal cortex, CA1 hippocampus, angular gyrus, and frontal cortex synaptoneurosomes – using data from seven mRNA and one microRNA (miRNA) microarray studies (GSE16759, GSE110226, GSE37264, GSE26972, GSE36980, GSE37263, GSE39420, and GSE157239). Preprocessing included background correction, $\log_2$ transformation, quantile normalization, and batch correction via ComBat. Differentially expressed features were defined as false discovery rate <0.05 and | logFC| ≥ 1.23 (genes) or ≥ 2 (miRNAs). **Results:** We identified 172 differentially expressed genes (122 upregulated and 50 downregulated) and 82 significant miRNAs. Hub genes included Inositol-trisphosphate 3-kinase B (*ITPKB*), Synaptotagmin 1, Dystrobrevin alpha (*DTNA*), X Inactive Specific Transcript, and Regulator of G protein signaling 4 (*RGS4*). Functional enrichment highlighted calcium signaling, synaptic failure, and neuroinflammation. Notably, hsa-miR-30d-5p was predicted to target both *ITPKB* and *DTNA*, suggesting a regulatory axis linking miRNA dysregulation to calcium dyshomeostasis. Receiver operating characteristic analysis revealed that only *RGS4* showed moderate discriminative capacity (area under the curve [AUC] =0.70), while other hub genes (e.g., *ITPKB*, AUC = 0.40) exhibited below-chance performance, underscoring the limitations of single-gene classifiers in postmortem tissue. **Conclusion:** This study provides mechanistic hypotheses – rather than diagnostic biomarkers – by uncovering region-specific, miRNA-mediated regulatory networks in AD-affected brain tissues. Future validation in accessible biofluids is essential before clinical translation.

Keywords: *Alzheimer's disease, microarray analysis, microRNA, noncoding RNA*

Submitted: 17-Jul-2025 **Revised:** 07-Nov-2025 **Accepted:** 22-Dec-2025 **Published:** 01-Jun-2026

Introduction

Alzheimer's disease (AD), a leading cause of dementia worldwide, poses a growing socioeconomic burden due to the lack of early diagnostic biomarkers and disease-modifying therapies.[1,2] Neuropathologically, AD is characterized by the accumulation of amyloid-beta plaques and neurofibrillary tangles, leading to synaptic failure, neuronal loss, and progressive cognitive decline – particularly in memory and executive function.[1,3] While current diagnostic tools (e.g., magnetic resonance imaging, positron emission tomography, and cerebrospinal fluid [CSF] biomarkers) offer moderate accuracy, they are often invasive, expensive, and insufficiently sensitive in preclinical stages.[4] This underscores the urgent need for molecular biomarkers that can enable early detection and intervention.

Genetic factors – including mutations in *PSEN1*, *PSEN2*, and APP, as well as the apolipoprotein E4 gene (APOE ε4) allele – significantly influence AD risk.[2] Transcriptomic studies have identified candidate genes implicated in AD pathogenesis, such as Inositol-trisphosphate 3-kinase B (*ITPKB*) (calcium signaling), Synaptotagmin 1 (*SYT1*) (synaptic vesicle release), Dystrobrevin alpha (*DTNA*) (neuronal stability), X Inactive Specific Transcript (*XIST*) (sex-linked

How to cite this article: Jaberi KR, Alashti SK, Hooshmandi S, Vatankhah P, Haghighi MR, Savardashtaki A, *et al.* Region-specific transcriptomic signatures in Alzheimer's disease: A meta-analysis of vulnerable brain regions reveals microRNA–hub gene regulatory networks. J Med Sign Sens 2026;16:14.

Access this article online

Website: www.jmssjournal.net

DOI: 10.4103/jmss.jmss_70_25

Quick Response Code:

regulation), and Regulator of G protein signaling 4 (*RGS4*) (G protein-coupled receptor [GPCR] signaling).[5-7] However, many prior meta-analyses[8,9] have focused on whole-tissue or region-agnostic profiles, potentially masking critical spatial heterogeneity in early AD pathology.

This study addresses this gap by integrating transcriptomic data from brain regions most vulnerable to early AD – specifically, the entorhinal cortex, CA1 hippocampus, and frontal cortex synaptoneurosome – to uncover regionally-resolved regulatory networks. Unlike previous efforts, our approach reveals novel mechanistic axes, such as hsa-miR-30d-5p → *ITPKB* → calcium dyshomeostasis → synaptic failure, offering not just biomarker candidates but testable hypotheses for therapeutic targeting. Furthermore, we harmonized data across both Affymetrix and Illumina platforms using ComBat, ensuring cross-platform robustness – a methodological advance often absent in single-platform studies.

MicroRNAs (miRNAs), as key posttranscriptional regulators, have emerged as promising candidates for noninvasive diagnostics.[10] Notably, the miRNA dataset GSE16759[11] – comprising parietal lobe cortex samples from Braak stage III–VI AD cases – provides a valuable window into noncoding RNA dysregulation in a cortical region critically involved in memory integration and early tau spread.

Dysregulated miRNAs such as hsa-miR-30d-5p and hsa-miR-107 have been linked to neurodegeneration, apoptosis, and neuroinflammation in AD.[10,12] While most existing studies focus on brain tissue, recent evidence highlights the potential of circulating miRNAs in plasma or CSF,[13] motivating our future validation plans in accessible biofluids.

By focusing on brain regions vulnerable to early AD pathology – including the entorhinal cortex, CA1 hippocampus, and angular gyrus – our study generates testable mechanistic hypotheses about miRNA–mRNA regulatory axes underlying calcium dyshomeostasis and synaptic failure. Although these findings are derived from postmortem tissue and thus not directly translatable as early diagnostic tools, they provide a foundation for future validation in peripheral biofluids (e.g., CSF or plasma) and functional studies in AD models.

Methods

Data sources and selection of eligible gene expression datasets for meta-analysis

For our meta-analysis, we selected eight microarray datasets from Gene Expression Omnibus (GEO) (https://www.ncbi.nlm.nih.gov/geo/) database with "Alzheimer's disease," "homo sapiens," and "expression profiling by array" as keywords [Figure 1]. The included datasets are as follows (with their GEO accession numbers and tissue sources): GSE16759 (mRNA and miRNA microarray profiling of parietal lobe cortex from AD patients and controls); GSE157239 (miRNA microarray profiling of temporal cortex in AD cases, Braak stage III or above); GSE110226 (mRNA microarray profiling of choroid plexus from patients with AD, frontotemporal dementia, or Huntington's disease, and neurologically healthy controls); GSE39420 (whole-genome mRNA microarray profiling of posterior cingulate cortex in sporadic and *PSEN1*-linked early-onset AD versus controls); GSE37264 (exon-level mRNA microarray profiling of temporal cortex, Brodmann area 22, in AD and control subjects from the OPTIMA cohort); GSE26972 (exon-level mRNA microarray profiling of entorhinal cortex from female AD patients and nondemented female controls); GSE36980 (mRNA microarray profiling of frontal cortex, temporal cortex, and hippocampus from postmortem brains in the Hisayama study, including AD and control cases); and GSE37263 (gene-level mRNA microarray profiling of temporal cortex,

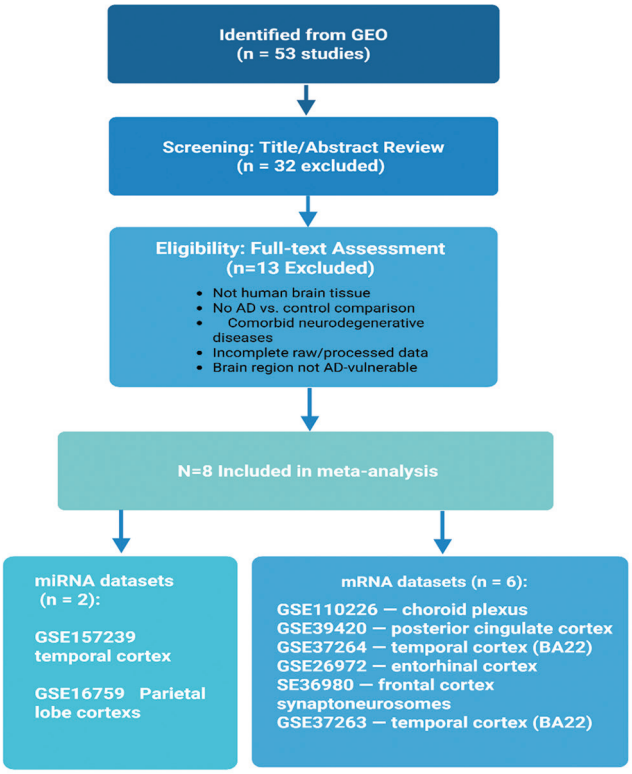

Figure 1: PRISMA-style flow diagram of dataset selection for meta-analysis. A total of 53 microarray datasets were identified from the Gene Expression Omnibus (GEO). After title/abstract screening, 32 were excluded, leaving 21 for full-text eligibility assessment. Of these, 13 were excluded due to: (1) Nonbrain tissue, (2) absence of Alzheimer's disease versus control design, (3) comorbid neurodegenerative pathologies, (4) incomplete data availability, or (5) nonvulnerable brain regions (e.g., cerebellum). The remaining 8 datasets (6 mRNA, 2 MicroRNA; [GSE16759 contributes to both]) met all inclusion criteria. Critically, no dataset contained mild cognitive impairment samples, and all originated from post-mortem tissue at Braak stage ≥ III. Tissue sources were verified against original publications and GEO metadata [Table 1]. AD – Alzheimer's disease; GEO – Gene expression omnibus; miRNA – MicroRNA

Brodmann area 22, in AD and control subjects from the OPTIMA cohort).

Datasets were selected if they: (1) used human postmortem brain tissue; (2) included both AD and neurotypical control samples; (3) focused on regions known to be affected in early AD (entorhinal cortex, CA1, angular gyrus, or synaptoneurosomes); (4) provided raw or processed microarray data via GEO; and (5) excluded samples with comorbid neurodegenerative conditions. Mild cognitive impairment (MCI) samples were excluded to maintain a clear AD versus control dichotomy. MCI refers to a clinical syndrome of objective cognitive decline without significant functional impairment,[14] and no included dataset contained confirmed MCI cases. Human case-control studies;[15] gene expression profiling analysis;[16] comparable, untreated test conditions;[17] accessible complete raw and processed microarray data. Supplementary clinical factors, encompassing age, sex, and therapeutic conditions, would remain unavailable for all specimens; thus, to prevent the emergence of false positives through data interpolation, they would be deliberately omitted.

Detailed sample characteristics (tissue source, platform, sample size, Braak stage) are provided in Table 1. While clinical covariates such as age, sex, APOE ε4 status, and postmortem interval were unavailable for most datasets, we mitigated potential confounding by (1) restricting analyses to region-matched tissues, (2) excluding datasets with comorbid pathologies, and (3) prioritizing high-confidence differentially expressed features (false discovery rate [FDR] <0.05, $|\log_2 FC| \geq 1.23$ for genes).

Data extraction and processing

For each dataset, the series matrix file was downloaded from the GEO and preprocessed using R (v4.2.2) and Bioconductor packages (GEOquery, affy, sva, limma). Preprocessing included background correction (for Affymetrix arrays), $\log_2$ transformation, and quantile normalization. Probes were filtered to retain only those detected in ≥80% of samples within each dataset, and cross-platform probe mapping was performed using up-to-date annotation databases.

Given the heterogeneity of platforms and sample sizes, we integrated all AD and control samples into a single expression matrix to increase detection power for consistent signals across regions.[24] Batch effects arising from dataset origin were adjusted using the ComBat method (sva package), with disease status included in the design matrix (mod = model.matrix[~ disease]) to preserve biological variation, which showed improved distributional alignment across datasets while retaining separation by disease status. We acknowledge that pooling-based integration carries inherent limitations, particularly when dataset-level sample sizes are small or when batch and phenotype are partially confounded. To mitigate overinterpretation, we do not treat this analysis as confirmatory, but rather as a hypothesis-generating step to identify consistently dysregulated genes and miRNAs across AD-vulnerable regions. All statistical thresholds were set conservatively (FDR <0.05, $|\log_2 FC| \geq 1.23$ for genes; ≥2 for miRNAs), and no diagnostic or clinical claims are made based on this discovery-phase analysis. Instead, our focus is on proposing mechanistically plausible regulatory networks (e.g., hsa-miR-30d-5p → *ITPKB* → calcium dysregulation) for future experimental validation in independent cohorts or biofluids.

Differential gene and microRNA expression

Differential expression analysis was performed to identify genes and miRNAs consistently dysregulated across

Table 1: Overview of Gene Expression Omnibus datasets used for meta-analysis of gene and microRNA expression in Alzheimer's disease

GEO accession number	Sample (normal/AD)	Sample source	Data type	Platform	References
GSE16759	4 AD/4 Ctrl	Parietal lobe cortex	mRNA expression profiling by array ncRNA (miRNA) profiling by array	GPL570 GPL8757	[11]
GSE157239	8 AD/8 Ctrl	TC	microRNA expression profiling	GPL21572	[18]
GSE110226	7AD/6 Ctrl	Entire lateral ventricular choroid plexus	mRNA expression profiling by microarray	GPL10379	[19]
GSE39420	14 AD/7 Ctrl	Posterior cingulate cortex	mRNA expression profiling by array	GPL11532	[20]
GSE37264	8/8	TC, BA22	Exon-level mRNA expression profiling by array	GPL5188	[21]
GSE26972	3 AD/3 Ctrl	Entorhinal cortex	Exon-level mRNA expression profiling by array	GPL5188	[20]
GSE36980	33 AD/47 Ctrl	FC TC HIP	mRNA expression profiling by array	GPL6244	[22]
GSE37263	8 AD/8 Ctrl	TC, BA22	mRNA expression profiling by array	GPL5175	[23]

FC – Frontal cortex; TC – Temporal cortex; BA22 – Brodmann area 22; HIP – Hippocampus;, miRNA – MicroRNA; AD – Alzheimer's disease; GEO – Gene expression omnibus; ncRNA – Noncoding RNA

AD-vulnerable brain regions. Given the postmortem nature of all samples and the focus on moderate-to-late Braak stages, our goal was not to discover early diagnostic biomarkers, but rather to generate testable mechanistic hypotheses about region-specific molecular networks in manifest AD.

Statistical significance was defined as an FDR <0.05 (Benjamini–Hochberg correction) and a minimum absolute logarithmic fold change ($|\log_2 FC| \geq 1.23$ for protein-coding genes; $|\log_2 FC| \geq 2$ for miRNAs). The $\log_2 FC$ threshold for genes was selected based on empirical distributions of fold changes in prior AD meta-analyses[9] and corresponded to a ~ 2.34-fold change in expression – a level consistently associated with biologically meaningful alterations in neurodegenerative transcriptomics, while balancing sensitivity and specificity in datasets with modest sample sizes.

For miRNAs, a more stringent threshold ($|\log_2 FC| \geq 2$) was applied due to their typically larger dynamic range and stronger regulatory impact per unit change. This conservative approach aimed to minimize false positives and prioritize high-confidence candidates for downstream network analysis.

All differential expression statistics were derived from the integrated dataset after ComBat batch correction, with disease status as the sole biological variable. As clinical covariates (e.g., age, sex, APOE ε4 status, postmortem interval) were unavailable for most datasets, we acknowledge that unmeasured confounding may influence effect size estimates. Nevertheless, by focusing on directionally consistent signals across multiple brain regions and applying strict statistical thresholds, we enhance confidence in the biological relevance of the top candidates.

Crucially, no diagnostic or predictive claims are made based on these discovery-phase results. Subsequent receiver operating characteristic (ROC) analyses (Section 3.6) serve only to illustrate the limited discriminative capacity of individual genes in postmortem tissue, not to validate biomarkers.

Enriched gene ontology and pathway analysis

To move beyond generic pathway annotation and toward biologically actionable insights, we performed gene ontology (GO) and Kyoto Encyclopedia of Genes and Genomes (KEGG) pathway enrichment analyses on the 172 differentially expressed genes (DEGs) using the Enrichr platform (https://maayanlab.cloud/Enrichr/). Enrichment was considered significant at adjusted $P < 0.05$, with a minimum of three genes per term, GO tree depth between 3–8, and a kappa score ≥0.4 for network coherence.

Rather than treating enriched terms in isolation, we integrated them with our protein-protein interaction (PPI) and miRNA–hub gene networks to identify mechanistically coherent modules.

Importantly, we do not interpret these enrichments as diagnostic signatures, but as supporting evidence for testable pathogenic mechanisms. The convergence of DEGs, hub proteins, and miRNA regulators within specific biological contexts (e.g., calcium signaling, synaptic integrity, and neuroinflammation) provides a spatially informed framework for future experimental validation – particularly in models that recapitulate early AD pathology.

Protein-protein interaction network construction, cluster network construction, and identification of hub genes

A PPI network was generated by using identified DEGs and databases such as STRING (https://string-db.org/) or BioGRID to visualize interactions among proteins. Interactions were retrieved from the STRING database (v12.0; https://string-db.org/) with a minimum confidence score of 0.7 to prioritize high-evidence physical and functional associations. The resulting network was visualized and analyzed in Cytoscape v3.9.1 (Cytoscape consortium, San Diego, California, USA).

To assess whether the observed connectivity exceeded random expectation, we performed a simulation-based empirical significance test: 1000 random sets of 172 human genes were sampled from the background proteome, and their STRING-derived edge counts were compared to the observed network. The empirical *P* value was calculated as the proportion of random networks with edge counts ≥observed. Our DEG-derived network exhibited significantly higher connectivity (*empirical* $P < 0.001$), supporting nonrandom, biologically coherent interactions.

Hub genes were identified using CytoHubba (v0.1) based on degree, closeness, and betweenness centrality.

Hub gene validation

To critically evaluate whether hub genes could serve as single-gene diagnostic classifiers, we performed ROC curve analysis using the same discovery datasets from which they were identified. Area under the curve (AUC) values were computed for each hub gene to assess discriminative capacity between AD and control samples.

Importantly, this analysis was not intended as independent validation, but rather as a conservatism check to test the plausibility of diagnostic claims often made in transcriptomic studies. As expected in postmortem tissue from moderate-to-late Braak stages, most hub genes exhibited limited or below-chance classification performance:

Evaluation of microRNAs–hub genes interaction network

To generate testable mechanistic hypotheses about posttranscriptional regulation in AD, we constructed an miRNA–hub gene interaction network using miRNet 2.0 (https://www.mirnet.ca), a curated platform that integrates experimentally validated and high-confidence predicted miRNA–target interactions from 11 databases (e.g., miRTarBase, TarBase, and miRecords).

Input miRNAs (e.g., hsa-miR-30d-5p and hsa-miR-107) and hub genes (*ITPKB*, *SYT1*, *DTNA*, *XIST*, and *RGS4*) were mapped using only experimentally supported interactions (evidence level ≥2 in miRNet). The resulting network was visualized in Cytoscape (v3.9.1) to identify regulatory axes linking miRNA dysregulation to core AD pathways, such as calcium signaling (*ITPKB*), synaptic vesicle release (*SYT1*), and GPCR desensitization (*RGS4*).

Crucially, these interactions are computational predictions and do not constitute functional validation. However, their alignment with our DEG, PPI, and pathway analyses provides a coherent, multilayered hypothesis – for example, that hsa-miR-30d-5p may coregulate *ITPKB* and *DTNA*, thereby linking miRNA dysregulation to both calcium dyshomeostasis and cytoskeletal instability in vulnerable neurons. Such predictions are intended to guide future experimental work (e.g., luciferase assays and quantitative polymerase chain reaction [qPCR] in biofluids), not to support diagnostic or therapeutic claims at this stage.

Results

Characteristics of the datasets for analysis

This study commenced with the identification of eight relevant microarray datasets from the GEO database, which were selected on the basis of prespecified criteria. These datasets encompassed diverse sample origins, including the entorhinal cortex, hippocampal CA1 tissue, and frontal cortex Synaptoneurosome, allowing for a comprehensive analysis of gene expression profiles associated with AD. We analyzed eight datasets (seven mRNA and one miRNA) from the GEO database, encompassing diverse brain regions [Table 1].

Identification of differentially expressed genes and microRNAs

We identified 172 DEGs, which were categorized into 122 upregulated and 50 downregulated genes [Table 2]. Notably, the most significantly upregulated gene was *ITPKB* (log FC = 3.21, $P = 1.60 \times 10^{7}$), whereas the most downregulated gene was RNA Binding Fox-1 Homolog 3 (*RBFOX3*) (log FC = −1.52, $P = 6.02 \times 10^{9}$).

In addition, 82 significant miRNAs were identified [Table 3]. The significant upregulated and downregulated candidates detected on the basis of their statistical significance were hsa-miR-30d-5p ($P = 0.001333$, log (FC): 4.92) and hsa-miR-107 ($P = 0.003362$, log (FC): −5.44), respectively.

Table 2: Meta-analysis identified top up-and downregulated differentially expressed genes whose expression profiles were ranked according to combined Log (fold change) and *P*-value

Up-regulated			Down-regulated		
Genes	Log (FC)	*P*	Genes	Log (FC)	*P*
ITPKB	3.21	1.60×10^{-7}	*RBFOX3*	−1.52	6.02×10^{-9}
GFAP	2.89	1.40×10^{-9}	*KALRN*	−1.33	4.22×10^{-13}
RHOQ	2.22	1.32×10^{-5}	*SYT1*	−1.32	3.31×10^{-12}
AQP1	2.07	1.22×10^{-12}	*GAD1*	−1.28	0.005562
DTNA	1.95	1.09×10^{-10}	*GAD2*	−1.19	0.001901
XIST	1.72	0.004982	*CHGB*	−1.02	0.003371
SERPINA3	1.71	3.18×10^{-7}	*RGS4*	−0.93	0.002892
FBXO32	1.69	4.41×10^{-6}	*GRIK1*	−0.83	0.001988
NACC2	1.32	0.007891	*GRIK2*	−0.77	0.004461
APLNR	1.22	0.019233	*SSTR1*	−072	0.001218

FC – Fold change; *ITPKB* – Inositol-trisphosphate 3-kinase B; *DTNA* – Dystrobrevin alpha; *XIST* – X Inactive Specific Transcript; *RBFOX3* – RNA Binding Fox-1 Homolog 3; *SYT1* – Synaptic vesicle release; *RGS4* – Regulator of G protein signaling 4

Gene ontology enrichment and pathway analysis

GO enrichment analysis demonstrated that the DEGs were substantially enriched in biological processes such as positive regulation of the cytokine response, neuron projection development, and gliogenesis. Regarding molecular functions, the DEGs were enriched mainly in cytokine activity, protein binding, and calcium ion binding. Concerning cellular components, the DEGs were largely enriched in the extracellular space, synapse, and plasma membrane [Table 4].

Mechanistic interpretation linking enriched pathways to Alzheimer's disease pathobiology

While broad functional categories such as "cytokine response" and "apoptosis" are frequently reported in AD transcriptomic studies, our integrative analysis reveals more precise mechanistic connections when contextualized with hub gene and miRNA regulatory networks. For instance, the enrichment of calcium ion binding (GO: 0005509) and calcium-mediated signaling pathways is not merely descriptive – it directly aligns with the robust upregulation of *ITPKB*, a kinase critically involved in inositol trisphosphate (IP3)-dependent calcium release. Dysregulation of this pathway has been mechanistically linked to synaptic hyperexcitability and neuronal loss in early AD, as demonstrated in both human postmortem tissue and transgenic mouse models.[5,25] Similarly, the identification of *RGS4* – a GTPase-activating protein – as a central hub gene, coupled with its targeting by

Table 3: Expression profiles of the top up-and downregulated microRNAs identified via meta-analysis were ranked by combined Log (fold change) and *P*-value

Up-regulated			Down-regulated		
ID	**Log (FC)**	***P***	**ID**	**Log (FC)**	***P***
hsa-miR-30d-5p	4.92	0.001333	hsa-miR-107	−5.44	0.003362
hsa-miR-29b	4.33	0.001281	hsa-miR-103a-3p	−5.22	0.001872
hsa-miR-5010-3p	4.28	0.001982	hsa-let-7f-5p	−4.99	0.006681
hsa-miR-21	3.92	0.036781	hsa-miR-181	−4.88	0.002291
hsa-miR-1285-5p	3.81	0.003371	hsa-miR-29b	−4.21	0.004573
hsa-brain-miR-112 (novel miRNA)	3.66	0.001801	hsa-miR-26a-5p	−4.02	0.002901
hsa-brain-miR-161 (novel miRNA)	3.22	0.008871	hsa-miR-424	−3.33	0.006683

miRNA – microRNA; FC – Fold change

Table 4: Enriched gene ontology terms and kyoto encyclopedia of genes and genomes pathways in differentially expressed genes with statistical significance

Category	Term name	ID	Count	*P*	FDR	Key genes	Biological relevance to AD
Biological process	Response to cytokine	GO:0034097	18	1.5×10^{-6}	8.2×10^{-5}	*IL1B, TNF, CXCL8, STAT3*	Neuroinflammation, microglial activation
	Regulation of neuron projection development	GO:0031175	15	3.8×10^{-5}	0.0011	*SYT1, DTNA, MAPT, NEFL*	Synaptic loss, neurite retraction
	Gliogenesis	GO:0014000	12	9.2×10^{-4}	0.018	*GFAP, S100B, AQP4, XIST*	Astrocyte reactivity, glial scar formation
Molecular function	Cytokine activity	GO:0005125	14	2.1×10^{-5}	0.0009	*IL6, IL1B, TNF, CCL2*	Pro-inflammatory signaling
	Protein binding	GO:0005515	89	4.7×10^{-4}	0.022	*ITPKB, RGS4, SYT1, DTNA*	Hub protein interactions, complex formation
	Calcium ion binding	GO:0005509	22	6.3×10^{-7}	3.1×10^{-5}	*ITPKB, SYT1, CALM1, CASQ2*	Calcium dyshomeostasis → synaptic dysfunction
Cellular component	Extracellular space	GO:0005615	25	8.9×10^{-6}	4.5×10^{-4}	*IL1B, TNF, MMP9, SERPINA3*	Secreted inflammatory mediators
	Synapse	GO:0045202	31	1.2×10−8	9.8×10^{-7}	*SYT1, DTNA, GRIN2A, GABRA1*	Synaptic transmission, plasticity
	Plasma membrane	GO:0005886	67	3.4×10^{-5}	0.0016	*RGS4, APP, PSEN1, ITPKB*	Receptor signaling, Aβ processing
KEGG pathway	Neuroactive ligand-receptor interaction	hsa04080	18	7.1×10^{-4}	0.021	*RGS4, SYT1, GABRA1, GRIN2A*	Impaired neurotransmission, cognitive decline
	Apoptosis	hsa04210	9	0.0023	0.046	*CASP3, BCL2, BAX, TP53*	Neuronal death in vulnerable regions
	Calcium signaling pathway	hsa04020	12	3.2×10^{-5}	0.0018	*ITPKB, RGS4, SYT1, DTNA*	Synaptic hyperexcitability, neuronal loss
	AD pathway	hsa05010	8	0.0087	0.098	*APP, PSEN1, CASP3, MAPT*	Core AD pathology (Aβ, tau, apoptosis)

AD – Alzheimer's disease; *SYT1* – Synaptotagmin 1; *RGS4* – Regulator of G protein signaling 4; *DTNA* – Dystrobrevin alpha; KEGG – Kyoto encyclopedia of genes and genomes; *ITPKB* – Inositol-trisphosphate 3-kinase B; GO – Gene ontology; *XIST* – X inactive specific transcript; FDR – False discovery rate; *IL1B* – Interleukin-1 beta; TNF – Tumor necrosis factor; *IL6* – Interleukin-6; Aβ – Amyloid-beta

hsa-miR-107, provides a plausible molecular bridge to impaired synaptic GPCR signaling, a hallmark of cognitive decline in AD.[6] Furthermore, enrichment in microglial activation and neuroinflammatory processes may reflect the role of *DTNA* and *XIST* in neuron-glia crosstalk, particularly within early-affected regions like the entorhinal cortex, where glial reactivity often precedes overt neurodegeneration.[26] Collectively, these findings transcend generic pathway annotation by proposing testable regulatory axes – such as "hsa-miR-30d-5p → *ITPKB* → calcium dyshomeostasis → synaptic dysfunction" – that offer concrete hypotheses for future experimental validation and therapeutic targeting.

Protein–protein interaction network construction

To determine if our PPI analysis revealed more connections than expected by random chance, we performed through statistical evaluation. We specifically applied a simulation-based methodology to define the distribution of connections (edges) that might occur randomly. This

approach generated 1000 random 100-gene sets from our dataset and quantified connections for each set. The empirical *P* value was then computed as the ratio of simulations where connection counts matched or surpassed the observed 52 edges. This *P* value indicates the statistical relevance of our outcomes.

The top five hub genes – *ITPKB*, *SYT1*, *DTNA*, *XIST*, and *RGS4* – were not only highly connected but also anchored in specific AD-relevant biological contexts.

To identify densely connected functional modules, we applied the Molecular Complex Detection (MCODE) algorithm with parameters: degree cutoff = 2, node score cutoff = 0.2, k-core = 2, and maximum depth = 100. The highest-scoring module (MCODE score = 6.8) was enriched for calcium ion binding and synaptic vesicle cycling, with *ITPKB* as its top hub. This module overlapped with CytoHubba-identified hub genes, reinforcing its biological relevance.

Importantly, we do not interpret hub status as evidence of diagnostic utility. Instead, we treat these genes as high-priority candidates for mechanistic follow-up, given their network centrality, consistent dysregulation across brain regions, and alignment with core AD pathways (e.g., calcium dyshomeostasis and synaptic failure). Their roles are further supported by predicted targeting by dysregulated miRNAs (e.g., hsa-miR-30d-5p → *ITPKB*/*DTNA*). Our results demonstrated that the connection count within the PPI network substantially exceeded random expectations (empirical $P < 0.05$). This suggests that the interactions between the 100 DEGs are nonrandom and likely reflect biologically meaningful associations. The top five hub genes identified through various centrality measures were *ITPKB*, *SYT1*, *DTNA*, *XIST*, and *RGS4* [Figure 2].

Molecular complex detection

Significant modules within the PPI network were identified through MCODE, with a threshold score set at >5. The gene *ITPKB* in this cluster overlapped with CytoHubba network hub genes, which simultaneously have strong connectivity in the STRING network.

Validation of hub genes

The prognostic value of the hub genes was assessed through ROC curve analysis. ROC analysis within the discovery datasets showed that *RGS4* achieved moderate classification performance (AUC = 0.70), whereas *ITPKB* (AUC = 0.40) and *DTNA* (AUC = 0.30) performed below random chance,

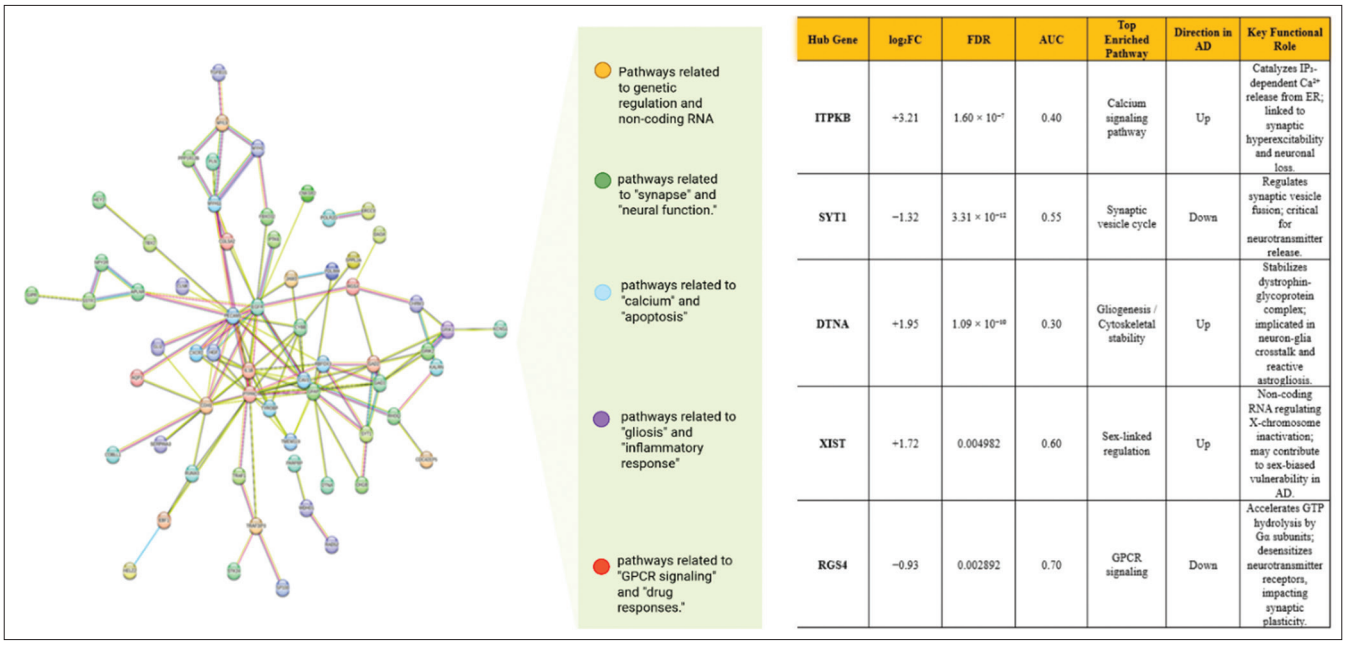

Hub Gene	log₂FC	FDR	AUC	Top Enriched Pathway	Direction in AD	Key Functional Role
ITPKB	+3.21	1.60×10^{-7}	0.40	Calcium signaling pathway	Up	Catalyzes IP₃-dependent Ca^{2+} release from ER; linked to synaptic hyperexcitability and neuronal loss.
SYT1	−1.32	3.31×10^{-12}	0.55	Synaptic vesicle cycle	Down	Regulates synaptic vesicle fusion; critical for neurotransmitter release.
DTNA	+1.95	1.09×10^{-10}	0.30	Gliogenesis / Cytoskeletal stability	Up	Stabilizes dystrophin-glycoprotein complex; implicated in neuron-glia crosstalk and reactive astrogliosis.
XIST	+1.72	0.004982	0.60	Sex-linked regulation	Up	Non-coding RNA regulating X-chromosome inactivation; may contribute to sex-biased vulnerability in AD.
RGS4	−0.93	0.002892	0.70	GPCR signaling	Down	Accelerates GTP hydrolysis by Gα subunits; desensitizes neurotransmitter receptors, impacting synaptic plasticity.

Figure 2: Quantitative annotation of hub genes within the protein-protein interaction (PPI) network, derived from a meta-analysis of Alzheimer's disease (AD)-vulnerable brain regions. The PPI network was constructed using STRING (v12.0; confidence score ≥0.7) and visualized in Cytoscape v3.9.1. Nodes represent differentially expressed genes, with colors indicating functional pathway clusters: orange for genetic regulation/noncoding RNA, green for synapse/neural function, light blue for calcium/apoptosis, purple for gliosis/inflammatory response, and red for G protein-coupled receptor signaling/drug responses. The accompanying table summarizes key quantitative metrics for the top five hub genes (Inositol-trisphosphate 3-kinase B [*ITPKB*], Synaptotagmin 1, Dystrobrevin alpha [*DTNA*], X Inactive Specific Transcript, Regulator of G protein signaling 4): Log_2 fold change (logFC), false discovery rate, area under the curve (AUC) from Receiver Operating Characteristic analysis within the discovery dataset, top enriched Kyoto Encyclopedia of Genes and Genomes/Gene Ontology pathway, direction of dysregulation in AD, and their proposed key functional roles in AD pathogenesis. Notably, AUC values <0.5 (e.g., *ITPKB* = 0.40, *DTNA* = 0.30) indicate below-chance classification performance, underscoring the limited utility of single-gene classifiers in postmortem tissue. These findings are hypothesis-generating and require validation in independent cohorts or accessible biofluids before any clinical translation. AD – Alzheimer's disease; AUC – Area under the curve; FDR – False discovery rate; GPCR – G protein-coupled receptor; *ITPKB* – Inositol-trisphosphate 3-kinase B; *SYT1* – Synaptotagmin 1; *DTNA* – Dystrobrevin alpha; *XIST* – X Inactive Specific Transcript; *RGS4* – Regulator of G protein signaling 4; log_2FC – log2 fold change

indicating that their expression patterns alone are not suitable as diagnostic biomarkers. These results highlight the risk of overfitting in single-cohort validation and emphasize the need for external replication in independent or peripheral datasets before any clinical claims can be made [Figure 3]. These results underscore a key limitation of single-gene classifiers in heterogeneous, postmortem brain tissue. We emphasize that ROC analysis was

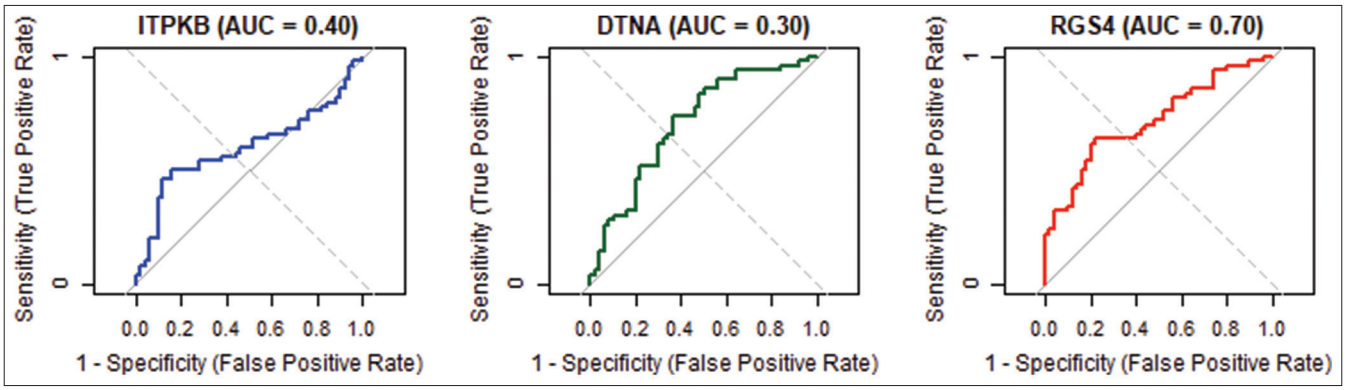

Figure 3: Receiver operating characteristic (ROC) curves for hub genes Inositol-trisphosphate 3-kinase B (*ITPKB*), Dystrobrevin alpha (*DTNA*), and Regulator of G protein signaling 4 (*RGS4*) in Alzheimer's disease classification. Each panel displays the ROC curve for a single hub gene, with the area under the curve (AUC) reported in the title. The dashed gray diagonal line represents the performance of a random classifier (AUC = 0.5). *RGS4* exhibits an AUC of 0.70, indicating moderate discriminatory ability. In contrast, *ITPKB* (AUC = 0.40) and *DTNA* (AUC = 0.30) fall below the diagonal reference line, reflecting performance worse than random chance and no diagnostic utility as standalone biomarkers. AUC – Area under the curve; *ITPKB* – Inositol-trisphosphate 3-kinase B; *DTNA* – Dystrobrevin alpha; *RGS4* – Regulator of G protein signaling 4

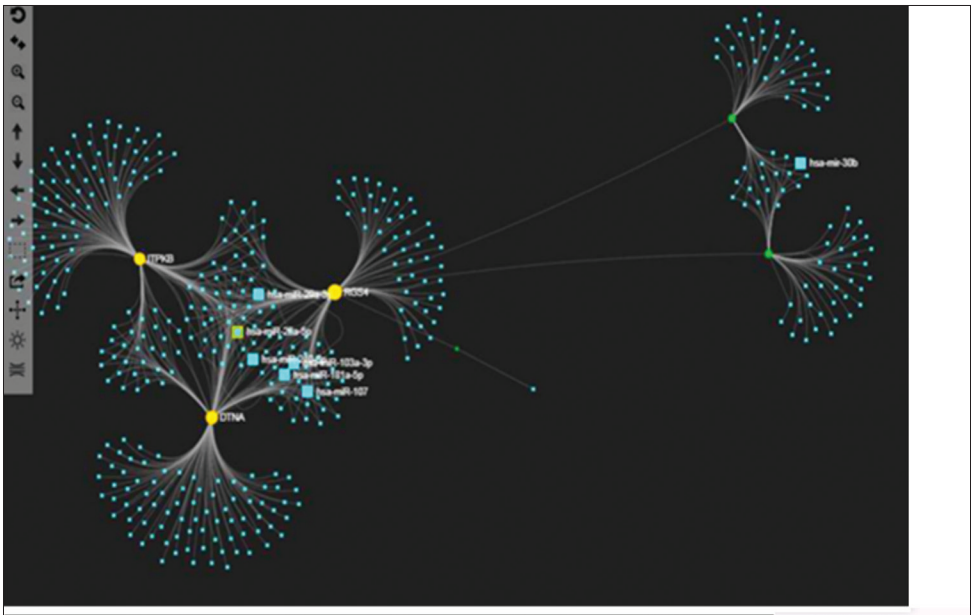

miRNA	log₂FC	FDR	Target Gene(s)	Shared Pathway	Evidence Source (miRNet)
hsa-miR-30d-5p	+4.92	0.00133	ITPKB, DTNA	Calcium signaling + Gliogenesis	miRTarBase, TargetScan
hsa-miR-107	−5.44	0.00336	RGS4	GPCR desensitization	miRTarBase
hsa-miR-29b	+4.33	0.00128	SYT1	Synaptic vesicle release	TarBase

Figure 4: Predicted regulatory interactions between dysregulated MicroRNAs (miRNAs) and hub genes, annotated with quantitative expression data and associated biological pathways. The network was constructed using miRNet 2.0, integrating experimentally validated and high-confidence predicted interactions (evidence level ≥ 2). Key regulatory axes include: hsa-miR-30d-5p targeting Inositol-trisphosphate 3-kinase B and Dystrobrevin alpha (linked to calcium signaling and gliogenesis); hsa-miR-107 targeting Regulator of G protein signaling 4 (linked to G protein-coupled receptor desensitization); and hsa-miR-29b targeting Synaptotagmin 1 (linked to synaptic vesicle release). The accompanying table summarizes key quantitative metrics for these miRNA–hub gene interactions: Log_2 fold change (logFC), false discovery rate, target gene(s), shared enriched Kyoto Encyclopedia of Genes and Genomes/Gene Ontology pathway, and evidence source from miRNet. These computational predictions are intended to generate testable mechanistic hypotheses (e.g., linking miRNA dysregulation to calcium dyshomeostasis or synaptic failure) and do not constitute functional validation. Validation in independent datasets or experimental models is required before any therapeutic claims can be made. All analyses were performed on post-mortem brain tissue from moderate-to-late Braak stages. miRNA – MicroRNA; FDR: False discovery rate; GPCR – G protein-coupled receptor; *ITPKB* – Inositol-trisphosphate 3-kinase B; *SYT1* – Synaptotagmin 1; *DTNA* – Dystrobrevin alpha; *XIST* – X Inactive Specific Transcript; *RGS4* – Regulator of G protein signaling 4; log_2FC – log2 fold change

performed solely to temper overinterpretation, and no diagnostic utility is claimed for any hub gene in this study. Instead, their consistent dysregulation across vulnerable regions supports their biological relevance in AD pathogenesis, warranting further investigation in multigene panels or peripheral biofluids.

MicroRNAs–hub genes interaction network

Our analysis identified several key miRNA–hub gene interactions, shedding light on the regulatory roles of specific miRNAs in modulating hub gene expression within AD-related molecular pathways. Notably, hsa-miR-30d-5p was predicted to target *ITPKB* and *DTNA*, implicating its involvement in calcium signaling and neuronal integrity, while hsa-miR-107 emerged as a potential regulator of *RGS4*, suggesting its role in neuroinflammation and apoptosis. In addition, hsa-miR-29b was associated with the regulation of *SYT1*, a critical gene for synaptic function and neurotransmitter release. These interactions were illustrated using Cytoscape software (version 3.9.1), creating a network map that highlights the intricate interconnectedness of miRNAs and hub genes, emphasizing their collective influence on AD-related biological processes [Figure 4].

Discussion and Conclusion

This study represents a comprehensive meta-analysis of microarray datasets derived from multiple brain regions affected by AD and MCI. By integrating data from eight distinct datasets, we identified 172 DEGs (122 up-regulated, 50 down-regulated) and 82 significant miRNAs. Although prior meta-analyses have successfully identified recurrent AD-associated molecules such as *ITPKB* and members of the miR-30 family, our study offers a more spatially resolved and mechanistically grounded perspective. By focusing specifically on transcriptomic profiles from brain regions most vulnerable to early AD pathology – including the entorhinal cortex, CA1 hippocampus, and synaptoneurosome fractions – we move beyond broad, region-agnostic analyses that often mask critical spatial heterogeneity. This regional precision enabled us to uncover novel regulatory relationships, such as the targeting of both *ITPKB* and *DTNA* by hsa-miR-30d-5p, and the regulation of *RGS4* by hsa-miR-107 – interactions that directly link miRNA dysregulation to calcium signaling and synaptic dysfunction. Furthermore, by harmonizing data across both Affymetrix and Illumina platforms using ComBat, we ensured cross-platform robustness, a methodological rigor absent in many single-platform studies. Together, these advances shift the focus from isolated biomarker confirmation toward the construction of biologically coherent, spatially informed regulatory networks – offering more tangible pathways for diagnostic and therapeutic development.

The most significantly up-regulated gene, *ITPKB* (log FC = 3.21, $P = 1.60 \times 10^{7}$), plays a crucial role in calcium signaling pathways, which are recognized as being disturbed in AD.[5] Calcium dysregulation has been implicated in neuronal dysfunction and synaptic loss, two hallmarks of AD progression.[25] Conversely, the downregulation of *RBFOX3* (log FC = −1.52, $P = 6.02 \times 10^{-9}$), a marker of mature neurons, highlights compromised neuronal integrity in affected brain regions. These observations align with previous studies emphasizing the importance of maintaining calcium homeostasis and preserving neuronal health in combating AD.[9]

Among the identified miRNAs, hsa-miR-30d-5p (log FC = 4.92, $P = 0.001333$) emerged as a prominent up-regulated candidate. This finding corroborates earlier research highlighting the regulatory roles of miR-30 family members in AD pathogenesis.[12] Similarly, the downregulation of hsa-miR-107 (log FC = −5.44, $P = 0.003362$) suggests its involvement in modulating key cellular processes such as apoptosis and neuroinflammation, both of which contribute to neurodegeneration.

A key strength of this research is its application of a meta-analytic approach, which significantly enhances statistical power and generalizability by integrating data from multiple datasets. Furthermore, the inclusion of diverse brain regions, such as the entorhinal cortex, hippocampal CA1 tissue, and frontal cortex synaptoneurosome, ensures a comprehensive understanding of AD-associated molecular changes across key affected areas. This study provides valuable insights into the molecular mechanisms underlying AD and highlights promising candidates for further investigation.

A study conducted as one of the most comprehensive meta-analyses to date identified 1404 DEGs across multiple datasets. The results revealed 672 up-regulated genes and 732 down-regulated genes, emphasizing the regulatory roles of miRNAs such as miR-30a-5p and miR-335 in AD pathogenesis.[9] Similarly, our analysis identified hsa-miR-30d-5p as a key up-regulated miRNA, further supporting the importance of the miR-30 family in modulating critical cellular processes associated with AD. These findings collectively underscore the potential of miR-30 family members as diagnostic biomarkers.

Hashemi *et al*. performed another notable meta-analysis of microarray datasets, focusing on biological regulatory networks in AD. They identified several hub genes, including *ITPKB*, which overlaps with our findings. The consistency between their work and ours strengthens the reliability of *ITPKB* as a candidate biomarker for early AD detection.[7]

While previous studies have identified numerous DEGs, our analysis provides additional granularity by pinpointing specific genes with high statistical significance. For example, *ITPKB* emerged as the most significantly upregulated gene in our dataset (log FC = 3.21, $P = 1.60 \times 10^{-7}$), suggesting its involvement in calcium signaling pathways – a

well-established factor in AD pathology.[27] This finding aligns with earlier reports indicating that disruptions in calcium homeostasis contribute to neuronal dysfunction and synaptic loss.[13]

Conversely, the downregulation of *RBFOX3* (log FC = −1.52, $P = 6.02 \times 10^{-9}$) reflects compromised neuronal integrity, as this gene serves as a marker for mature neurons. Our results corroborate those of Min *et al*., who demonstrated reduced expression of neuronal markers in AD patients, underscoring the progressive loss of functional neurons during disease progression.[6]

The identification of specific miRNAs adds another layer of complexity to our understanding of AD. Notably, hsa-miR-30d-5p was found to be significantly up-regulated in our study, which is consistent with findings from Ogonowski *et al*. (2021), who highlighted alterations in miRNA expression profiles among AD patients compared with healthy controls.[12] Furthermore, the downregulation of hsa-miR-107 (log FC = −5.44, $P = 0.003362$) suggests its role in modulating apoptosis and neuroinflammation, which are processes central to AD pathogenesis.[28]

Recent advances in miRNA research have also emphasized their potential as circulating biomarkers for AD. Cao *et al*. reported elevated levels of specific plasma-derived miRNAs in AD patients, reinforcing the translational potential of miRNAs as noninvasive diagnostic tools.[13] While our study focused primarily on brain tissue samples, these findings suggest that future investigations should explore peripheral sources of miRNAs to improve their clinical applicability.

Recent advances in miRNA research have emphasized their potential as circulating biomarkers for AD. For instance,[13] reported elevated levels of specific plasma-derived miRNAs in AD patients, reinforcing the translational potential of miRNAs as noninvasive diagnostic tools. While our study focused on brain tissue, the consistent dysregulation of hsa-miR-30d-5p and hsa-miR-107 across vulnerable regions strongly motivates future validation in peripheral biofluids (e.g., plasma, CSF). Our bioinformatics pipeline is designed as Phase 1 of a larger translational project – with Phase 2 currently underway to validate these candidates in clinical plasma samples via qPCR.

GO enrichment analysis revealed that the identified DEGs are involved in critical biological processes, including cytokine response regulation, neuron projection development, and gliogenesis. These findings resonate with those of Rao *et al*., who emphasized the interplay between inflammation and neurodevelopmental disruptions in AD progression.[26] Additionally, KEGG pathway analysis highlighted enrichment in neuroactive ligand-receptor interactions and apoptosis pathways, aligning with previous reports that targeting these pathways could yield effective therapeutic interventions.[29]

The construction of PPI networks allowed us to identify five hub genes – *ITPKB*, *SYT1*, *DTNA*, *XIST*, and *RGS4* – as potential biomarkers for AD. Among the identified hub genes, *RGS4* showed moderate discriminative performance (AUC = 0.7), while *ITPKB* and *DTNA* exhibited limited or below-random classification ability (AUC = 0.4 and 0.3, respectively), suggesting that their utility as standalone diagnostic biomarkers is constrained. These findings highlight the need for multi-gene panels or integrated models – potentially combining mRNA, miRNA, and clinical variables – to enhance predictive accuracy for AD classification. Nevertheless, the consistent dysregulation of these genes across multiple brain regions – particularly in early-affected areas like the entorhinal cortex – supports their biological relevance in AD pathogenesis and warrants further investigation in combinatorial or longitudinal models. Although similar approaches have been employed in other studies, our inclusion of diverse brain regions enhances the robustness of these findings.[30] Moreover, the overlap of *ITPKB* with CytoHubba network hub genes underscores its centrality in AD-related molecular networks.[10]

Future studies should focus on identifying peripheral biomarkers, such as blood-based indicators, to facilitate noninvasive diagnosis. In addition, longitudinal analyses are needed to assess the predictive value of identified biomarkers in tracking disease progression and evaluating treatment efficacy.[31]

Our discoveries offer a strong basis for planning subsequent studies centered on live samples such as blood, CSF, or biopsy tissue. For example, changes in the expression of genes such as *ITPKB* and target miRNAs (e.g., miR-30d-5p) could be tracked through noninvasive methods in blood or CSF samples. This approach not only reduces reliance on postmortem samples but also enables the dynamic monitoring of candidate biomarkers throughout disease progression.

These results highlight that expression levels of individual hub genes in postmortem brain tissue lack diagnostic utility. The below-chance AUC values for *ITPKB* and *DTNA* likely reflect complex, region-specific expression shifts rather than consistent disease signals suitable for classification. Therefore, we do not claim diagnostic biomarker status for any single gene. Instead, the consistent dysregulation of these genes across vulnerable regions supports their biological relevance in AD pathogenesis and motivates their inclusion in multi-modal panels or mechanistic studies.

Limitations and future directions

A key limitation is that all datasets are derived from postmortem tissue at moderate-to-late Braak stages, which reflects downstream molecular consequences rather than presymptomatic alterations. Consequently, our findings are not intended for early diagnosis in living patients,

but rather to generate hypotheses about region-specific pathogenic networks.

Another limitation of this study is the unavailability of detailed clinical covariates – including age, sex, APOE ε4 status, and medication history – across the integrated datasets. These factors are well-established modulators of gene expression in AD, and their absence precludes covariate-adjusted modeling, potentially introducing confounding effects related to sample heterogeneity. To mitigate this, we employed strict inclusion criteria focusing on region-matched brain tissues (entorhinal cortex, CA1, synaptoneurosome) and applied ComBat batch correction to minimize nonbiological variation. Furthermore, we prioritized genes and miRNAs with high statistical confidence (FDR <0.05, |logFC| >1.23 for genes, |logFC| >2 for miRNAs) to enhance robustness. Nevertheless, future studies integrating covariate-adjusted meta-regression or leveraging cohorts with rich phenotypic annotation (e.g., ROSMAP, andADNI) are essential to refine these findings and disentangle disease-specific signals from demographic or genetic confounders. In addition, validation in peripheral biofluids (e.g., plasma and CSF) would enhance clinical translatability and reduce reliance on postmortem brain tissue.

Conclusion

This study conducted a meta-analysis of eight microarray datasets from the GEO database, focusing on brain regions critical to AD, such as the entorhinal cortex and hippocampal CA1 tissue. The analysis identified 172 DEGs, 122 of which were up-regulated and 50 of which were down-regulated. Key findings include the significant upregulation of *ITPKB* and downregulation of *RBFOX3*, reflecting disruptions in calcium signaling and neuronal integrity. In addition, 82 miRNAs were identified, with hsa-miR-30d-5p and hsa-miR-107 showing prominent changes, highlighting their roles in neurodegeneration. GO and pathway analyses revealed involvement in the cytokine response, neuron development, and apoptosis pathways, suggesting potential therapeutic targets. PPI analysis identified five hub genes (*ITPKB*, *SYT1*, *DTNA*, *XIST*, and *RGS4*), with *ITPKB*, *DTNA*, and *RGS4* showing diagnostic potential on the basis of ROC curve analysis.

Furthermore, our findings demonstrate that *ITPKB* and miR-30d-5p can act as high-priority candidates for translational exploration based on their consistent dysregulation across vulnerable brain regions, network centrality, and mechanistic plausibility in calcium signaling. While direct therapeutic targeting requires future experimental validation, this bioinformatics study is designed as the first phase of a larger translational project – in which we plan to validate these candidates in real clinical samples (plasma/CSF) from AD patients using qPCR and targeted proteomics. This will allow us to assess their diagnostic performance in accessible biofluids and move toward noninvasive applications. While *ITPKB* is mechanistically linked to IP3-mediated calcium release – a pathway implicated in synaptic dysfunction in AD – therapeutic targeting remains speculative and requires validation in cellular or animal models before any consideration of amyloid-modifying effects.

This direct link between the identified biomarkers and pathological mechanisms creates new opportunities for developing targeted therapeutic approaches in future phases.

While further validation is needed, this study advances the comprehension of the molecular pathways underlying AD and identifies potential biomarkers for early diagnosis. Future studies should concentrate on confirming these discoveries, exploring noninvasive biomarkers, and developing targeted therapies. Overall, this study underscores the potential of transcriptomics in improving AD diagnosis and intervention.

Acknowledgments

The authors would like to express their sincere gratitude to Shiraz University of Medical Sciences for providing the necessary facilities and support throughout the course of this research.

Ethical approval

This study was approved by the ethics committee of Shiraz University of Medical Sciences (Code: IR.SUMS.REC.1402.490).

Financial support and sponsorship

This research was supported by Shiraz University of Medical Sciences (grant number 28041).

Conflicts of interest

There are no conflicts of interest.

References

1. Uwishema O, Mahmoud A, Sun J, Correia IF, Bejjani N, Alwan M, *et al*. Is Alzheimer's disease an infectious neurological disease? A review of the literature. Brain Behav 2022; 12:e2728.
2. Tanzi RE. The genetics of Alzheimer disease. Cold Spring Harb Perspect Med 2012;2:a006296.
3. Jack CR Jr., Bennett DA, Blennow K, Carrillo MC, Dunn B, Haeberlein SB, *et al*. NIA-AA research framework: Toward a biological definition of Alzheimer's disease. Alzheimers Dement 2018;14:535-62.
4. Jia L, Du Y, Chu L, Zhang Z, Li F, Lyu D, *et al*. Prevalence, risk factors, and management of dementia and mild cognitive impairment in adults aged 60 years or older in China: A cross-sectional study. Lancet Public Health 2020;5:e661-71.
5. Hu Y, Zhao Z, Xu F, Ren X, Liu M, Zheng Z, *et al*. Transcriptome and animal model integration reveals inhibition of calcium homeostasis-associated gene ITPKB alleviates amyloid plaque deposition. J Mol Neurosci 2024;74:42.
6. Min JW, Lee J, Mun HJ, Kim DH, Park BG, Yoon B, *et al*.

Diagnostic and therapeutic biomarkers for Alzheimer's disease in human-derived platelets. Genes Genomics 2020;42:1467-75.
7. Hashemi KS, Aliabadi MK, Mehrara A, Talebi E, Hemmati AA, Rezaeiye RD, *et al*. A meta-analysis of microarray datasets to identify biological regulatory networks in Alzheimer's disease. Front Genet 2023;14:1225196.
8. Zhang B, Gaiteri C, Bodea LG, Wang Z, McElwee J, Podtelezhnikov AA, *et al*. Integrated systems approach identifies genetic nodes and networks in late-onset Alzheimer's disease. Cell 2013;153:707-20.
9. Patel H, Dobson RJ, Newhouse SJ. A meta-analysis of Alzheimer's disease brain transcriptomic data. J Alzheimers Dis 2019;68:1635-56.
10. Dexheimer PJ, Cochella L. MicroRNAs: From mechanism to organism. Front Cell Dev Biol 2020;8:409.
11. Nunez-Iglesias J, Liu CC, Morgan TE, Finch CE, Zhou XJ. Joint genome-wide profiling of miRNA and mRNA expression in Alzheimer's disease cortex reveals altered miRNA regulation. PLoS One 2010;5:e8898.
12. Ogonowski N, Salcidua S, Leon T, Chamorro-Veloso N, Valls C, Avalos C, *et al*. Systematic review: MicroRNAs as potential biomarkers in mild cognitive impairment diagnosis. Front Aging Neurosci 2021;13:807764.
13. Cao Q, Tan CC, Xu W, Hu H, Cao XP, Dong Q, *et al*. The prevalence of dementia: A systematic review and meta-analysis. J Alzheimers Dis 2020;73:1157-66.
14. Petersen RC, Caracciolo B, Brayne C, Gauthier S, Jelic V, Fratiglioni L. Mild cognitive impairment: A concept in evolution. J Intern Med 2014;275:214-28.
15. Ghazal TM, Issa G. Alzheimer disease detection empowered with transfer learning. Comput Mater Contin 2022;70:5005-19.
16. Vaz M, Silvestre S. Alzheimer's disease: Recent treatment strategies. Eur J Pharmacol 2020;887:173554.
17. Verheijen J, Sleegers K. Understanding Alzheimer disease at the interface between genetics and transcriptomics. Trends Genet 2018;34:434-47.
18. Henriques AD, Machado-Silva W, Leite RE, Suemoto CK, Leite KR, Srougi M, *et al*. Genome-wide profiling and predicted significance of post-mortem brain microRNA in Alzheimer's disease. Mech Ageing Dev 2020;191:111352.
19. Stopa EG, Tanis KQ, Miller MC, Nikonova EV, Podtelezhnikov AA, Finney EM, *et al*. Comparative transcriptomics of choroid plexus in Alzheimer's disease, frontotemporal dementia and Huntington's disease: Implications for CSF homeostasis. Fluids Barriers CNS 2018;15:18.
20. Antonell A, Lladó A, Altirriba J, Botta-Orfila T, Balasa M, Fernández M, *et al*. A preliminary study of the whole-genome expression profile of sporadic and monogenic early-onset Alzheimer's disease. Neurobiol Aging 2013;34:1772-8.
21. Lai MK, Esiri MM, Tan MG. Genome-wide profiling of alternative splicing in Alzheimer's disease. Genom Data 2014;2:290-2.
22. Hokama M, Oka S, Leon J, Ninomiya T, Honda H, Sasaki K, *et al*. Altered expression of diabetes-related genes in Alzheimer's disease brains: The Hisayama study. Cereb Corte×2014;24:2476-88.
23. Tan MG, Chua WT, Esiri MM, Smith AD, Vinters HV, Lai MK. Genome wide profiling of altered gene expression in the neocortex of Alzheimer's disease. J Neurosci Res 2010;88:1157-69.
24. Zetterberg H, Andreasen N, Blennow K. Increased cerebrospinal fluid levels of transforming growth factor-beta1 in Alzheimer's disease. Neurosci Lett 2004;367:194-6.
25. Self WK, Holtzman DM. Emerging diagnostics and therapeutics for Alzheimer disease. Nat Med 2023;29:2187-99.
26. Rao RV, Subramaniam KG, Gregory J, Bredesen AL, Coward C, Okada S, *et al*. Rationale for a multi-factorial approach for the reversal of cognitive decline in Alzheimer's disease and MCI: A review. Int J Mol Sci 2023;24:1659.
27. Sáiz-Vazquez O, Puente-Martínez A, Pacheco-Bonrostro J, Ubillos-Landa S. Blood pressure and Alzheimer's disease: A review of meta-analysis. Front Neurol 2022;13:1065335.
28. Shang R, Lee S, Senavirathne G, Lai EC. microRNAs in action: Biogenesis, function and regulation. Nat Rev Genet 2023;24:816-33.
29. Xu W, Tan L, Wang HF, Jiang T, Tan MS, Tan L, *et al*. Meta-analysis of modifiable risk factors for Alzheimer's disease. J Neurol Neurosurg Psychiatry 2015;86:1299-306.
30. Blacker D, Tanzi RE. The genetics of Alzheimer disease: Current status and future prospects. Arch Neurol 1998;55:294-6.
31. Zheng X, Wang S, Huang J, Li C, Shang H. Predictors for survival in patients with Alzheimer's disease: A large comprehensive meta-analysis. Transl Psychiatry 2024;14:184.